The advantages of absorbed-dose calibration factors

D. W. O. Rogers
Institute for National Measurement Standards, National Research Council Canada, Ottawa, Canada K1A 0R6

(Received 26 December 1991; accepted for publication 17 June 1992)

A formalism for clinical external beam dosimetry based on use of ion chamber absorbed-dose calibration factors is outlined in the context and notation of the AAPM TG-21 protocol. It is shown that basing clinical dosimetry on absorbed-dose calibration factors N_D leads to considerable simplification and reduced uncertainty in dose measurement. In keeping with a protocol which is used in Germany, a quantity k_Q is defined which relates an absorbed-dose calibration factor in a beam of quality Q_0 to that in a beam of quality Q. For 38 cylindrical ion chambers, two sets of values are presented for N_D/N_X and N_{gas}/N_D and for k_Q for photon beams with beam quality specified by the TPR_{10}^{20} ratio. One set is based on TG-21's protocol to allow the new formalism to be used while maintaining equivalence to the TG-21 protocol. To demonstrate the magnitude of the overall error in the TG-21 protocol, the other set uses corrected versions of the TG-21 equations and the more consistent physical data of the IAEA Code of Practice. Comparisons are made to procedures based on air-kerma or exposure calibration factors and it is shown that accuracy and simplicity are gained by avoiding the determination of N_{gas} from N_X. It is also shown that the k_Q approach simplifies the use of plastic phantoms in photon beams since k_Q values change by less than 0.6% compared to those in water although an overall correction factor of 0.973 is needed to go from absorbed dose in water calibration factors to those in PMMA or polystyrene. Values of k_Q calculated using the IAEA Code of Practice are presented but are shown to be anomalous because of the way the effective point of measurement changes for ^{60}Co beams. In photon beams the major difference between the IAEA Code of Practice and the corrected AAPM TG-21 protocol is shown to be the P_{repl} correction factor. Calculated k_Q curves and three parameter equations for them are presented for each wall material and are shown to represent accurately the k_Q curve for all ion chambers in this study with a wall of that specified material and a thickness less than 0.25 g/cm^2. Values of k_Q can be measured using the primary standards for absorbed dose in photon beams.

I. INTRODUCTION

Most major primary standards laboratories have provided absorbed dose to water calibration factors in a ^{60}Co beam for up to 14 years. Nonetheless, despite the fact that the quantity of interest is absorbed dose to water, almost all current clinical dosimetry protocols, such as that of TG-21 of the AAPM[1] or the IAEA Code of Practice,[2] are based on the use of exposure or air-kerma calibration factors for ion chambers. The AAPM's TG-21 Protocol includes two sections (III H, VI B) on using absorbed-dose calibration factors, but they differ and have generally been ignored. Furthermore, these dosimetry protocols are very complicated because of the inherent difficulty of making the conversion from a quantity free-in-air to one in-phantom. This complexity is best demonstrated by considering the equations needed to use these protocols. A very terse summary of these equations is given in Appendix A.

To use the protocol a vast amount of data is needed along with considerable information about the physical characteristics of the ion chamber and detailed knowledge of the beam's quality. Many of these data, such as replacement correction factors and stopping-power ratios are derived from complex experimental measurements or calculations.[1,3]

In contrast to this complex chain of equations and data requirements is the intrinsically appealing concept of starting from an absorbed-dose to water calibration factor N_D. Henry pointed out in 1977 (Ref. 4) that one would expect that use of a calibration service for absorbed dose to water in a ^{60}Co beam would reduce considerably the uncertainty in obtaining the absorbed dose in higher-energy photon beams compared to starting from a ^{60}Co exposure calibration factor. Despite this expectation, very few clinics make use of absorbed-dose calibration services because dosimetry protocols are based on air-kerma calibration factors (the exceptions to this are the German dosimetry protocol[5] and a recent British protocol[6]). Furthermore, primary standards laboratories around the world are working toward developing primary standards for absorbed dose to water in accelerator beams. A wide variety of standards are being developed such as water-calorimeter based standards, chemical dosimetry standards, ionometric standards and graphite calorimeter standards, (see Ref. 7 for a review). Therefore, a very robust system of primary standards can be expected to be available in the next few years. As a result, the ICRU[8] has a report committee, chaired by Klaus Hohlfeld, which is both describing these various standards and is developing a formalism to allow effective use of these new standards. TG-51 of the AAPM has also

 0094-2405/92/51227-13$01.20

been charged with developing a new clinical dosimetry protocol.

This paper explores the implications of basing clinical dosimetry on absorbed dose to water calibration factors N_D. After concluding that it leads to significant simplifications, especially for photon beams, data are presented to allow the AAPM TG-21 protocol to be applied in this way.

II. USE OF AN ABSORBED-DOSE CALIBRATION FACTOR

A. Formalism

A formalism is developed here which is based on the approach used in the German protocol[5] and is being considered by the ICRU committee mentioned above. However, it is developed within the context and general notation of the AAPM TG-21protocol (which is summarized in Appendix A).

Given N_D^Q, the absorbed dose to water calibration factor for an ion chamber in a beam of quality Q (where beam quality can be specified in a variety of ways but for photon beams it is now common to use the measured TPR_{10}^{20} ratio in a 10×10 field[1,2]), then under reference conditions of field size and depth:

$$D_{\text{water}}^Q = MP_{\text{ion}}N_D^Q \quad \text{(Gy)}, \tag{1}$$

where D_{water}^Q is the absorbed dose to water at the location of the center of the ion chamber when it is absent; the ion chamber reading M has been corrected to reference conditions of temperature and pressure; and P_{ion} corrects for lack of complete charge collection in the user's beam and must be measured for each beam quality. This definition of N_D^Q is analogous to the definition of the exposure calibration factor N_X given by $X=MN_X$, where X is the exposure at the location of the center of the ion chamber (except that in the absorbed-dose equation the P_{ion} correction is made explicit because its effects are not negligible, unlike the normal case for exposure measurements). The following dose equation from the AAPM protocol also applies:

$$D_{\text{water}}^Q = MP_{\text{ion}}N_{\text{gas}}[P_{\text{wall}}P_{\text{repl}}(\bar{L}/\rho)_{\text{air}}^{\text{water}}]_Q \quad \text{(Gy)}, \tag{2}$$

where the factors are defined in Appendix A.

In the case where the absorbed-dose calibration factor $N_D^{Q_0}$ is known in some other beam quality Q_0, let k_Q be a factor which accounts for changes in the calibration factor between beam quality Q_0 and Q, i.e.,

$$N_D^Q = k_Q N_D^{Q_0} \quad \text{(Gy/C)}, \tag{3}$$

and from Eq. (1):

$$D_{\text{water}}^Q = MP_{\text{ion}}\, k_Q N_D^{Q_0} \quad \text{(Gy)}. \tag{4}$$

Equations (1) and (2) give

$$N_D^Q = N_{\text{gas}}[P_{\text{wall}}P_{\text{repl}}(\bar{L}/\rho)_{\text{air}}^{\text{water}}]_Q \quad \text{(Gy/C)}. \tag{5}$$

Eliminating N_{gas} from this equation by using the analogous equation for a beam of quality Q_0 allows one to solve for k_Q as given in Eq. 3:

$$k_Q = \frac{[P_{\text{wall}}P_{\text{repl}}(\bar{L}/\rho)_{\text{air}}^{\text{water}}]_Q}{[P_{\text{wall}}P_{\text{repl}}(\bar{L}/\rho)_{\text{air}}^{\text{water}}]_{Q_0}}. \tag{6}$$

The quantity k_Q relates the absorbed-dose calibration factor in a beam of quality Q to that for a beam of quality Q_0 in the same medium.

In this approach, all correction factors are gathered together and can be thought of as a single correction to account for the change in the absorbed-dose calibration factor with beam quality. From the user's point of view this is the simplest possible approach since it uses a correction factor k_Q which is conceptually very straightforward and yet takes into account all of the physics.

While it can rightly be argued that a lot of different physical effects have been collected in this one factor, it should be noted that: (i) k_Q can, in principle, be measured accurately by making use of the primary standards for absorbed dose to water which are being developed; (ii) it is generally a small correction for photon beams; (iii) Eq. (6) gives an explicit method for calculating k_Q in a manner equivalent to the AAPM TG-21protocol (and similar equations consistent with other protocols can obviously be developed).

The major advantage of using Eq. (4) as the basis of a dosimetry protocol is the simplicity of using it. This fact alone should reduce the number of errors involved in clinical dosimetry. Furthermore, the concept of k_Q is very straightforward which should make it much easier to teach and to learn. At the same time, this approach should reduce the uncertainties in dosimetry protocols for photon beams. Instead of needing the values of P_{wall}, $(\bar{L}/\rho)_{\text{air}}^{\text{med}}$ and P_{repl} at a given beam quality for a given detector, only the change in these values is needed as beam quality changes from Q_0 to Q and presumably these changes are better known than the absolute values as will be discussed below in Sec. III A. This advantage does not apply in the case of electron beams where a knowledge of more than changes in quantities is needed since the ratios involved are for different quantities. However, for both electron and photon beams, the use of absorbed-dose calibration factors as the starting point in the dosimetry chain means that there is no need to determine N_{gas} from an exposure or air-kerma calibration factor and hence there is no need to know the many factors required to determine it that way (i.e., as shown in Appendix A, cap thickness, cavity length, and the calibration beam factors K_{comp}, K_{wall} (or A_{wall}), $(\overline{\mu_{en}/\rho})_{\text{air}}^{\text{wall}}$, $(\bar{L}/\rho)_{\text{air}}^{\text{wall}}$, $(\overline{\mu_{en}/\rho})_{\text{air}}^{\text{cap}}$, $(L/\rho)_{\text{air}}^{\text{cap}}$, K_{st}, and K_{pn}).

One practical but real problem in applying dosimetry protocols is the need to use waterproofing sleeves which can have a non-negligible effect on the chamber response. This problem is also alleviated by using the k_Q approach, with the predicted corrections for waterproofing sleeves often halved as will be seen below.

In principle, Q_0 in Eq. (3) and elsewhere could be any beam quality for which an absorbed-dose calibration factor is available. However, in practical terms, even for those

standards laboratories with standards for accelerator beams, it is much easier to provide calibration factors for a ^{60}Co beam than for an accelerator beam. Furthermore, there are many primary and secondary standards laboratories without access to accelerators. Finally specification of beam quality is more complex and/or more critical for accelerator beams. Thus the most appropriate choice for Q_0 is a ^{60}Co beam, and that shall be assumed in the remainder of this paper.

Given the simplicity of this approach based on absorbed-dose calibrations and the general availability of ^{60}Co absorbed dose to water calibration services at standards laboratories, it is reasonable to develop dosimetry protocols based on this approach, as already done in Germany[5] and as being considered by TG-51 of the AAPM. However, in the short term it is possible to apply this approach in a manner which gives the values of the AAPM TG-21 protocol for the assigned dose. This is the subject of the next two sections.

B. Dosimetry in photon beams

A computer program, called PROT, has been written to calculate k_Q and other protocol related quantities for photon beams as a function of beam quality Q, for an arbitrary ion chamber in a phantom of water, PMMA, or polystyrene. The program is described in detail in Appendix B and an internal report[14] is available with extensive tables of values for all the ion chambers discussed in this paper. The program calculates k_Q using the equations and data of the original TG-21 protocol[1] or using the TG-21 equations with the more consistent physical data of the IAEA Code[2] (but note these values are not the values of k_Q obtained using the IAEA Code of Practice as shown below in Sec. VI). The results for an ion chamber in a water phantom are presented in Table I for the 27 cylindrical chambers presented in Gastorf *et al.*[9] and for an additional 11 chambers given in the IAEA Code of Practice. The calculation of k_Q values for a given ion chamber requires knowledge of the wall material, its wall thickness and the diameter of the cavity.

The k_Q values in Table I can be used directly with ^{60}Co absorbed dose to water calibration factors and Eq. (4) to determine the dose under reference conditions in a water phantom irradiated by a photon beam. The values of k_Q based on the IAEA data set are in principle more accurate. However, to maintain equivalence with the TG-21 protocol of the AAPM, the TG-21 values must be used. Unfortunately, the goal of equivalence to the TG-21 protocol is not achieved if an absorbed-dose calibration factor is used because the TG-21 protocol starts from an exposure calibration factor. In order to achieve the goal of complete equivalence to the AAPM TG-21 protocol and at the same time to allow use of the conceptually simpler k_Q formalism, Table I includes a column giving the TG-21 conversion from N_X to N_D (in a ^{60}Co beam) which is

$$\frac{N_D}{N_X}=\frac{N_{gas}}{N_X}\,[P_{wall}P_{repl}(\bar{L}/\rho)^{water}_{air}]_{^{60}Co} \quad \text{(Gy/R)}, \qquad (7)$$

where N_X is in R/C [divide N_D/N_X by 2.58×10^{-4} (C/kg)/R to get the result in Gy/(C/kg) for use with N_X in kg^{-1} when using the SI unit for exposure C/kg]. Using the values in the upper row for each chamber, one can start from an exposure calibration factor N_X, obtain the TG-21 equivalent value of N_D and then determine the absorbed dose in any quality beam using the tabulated k_Q values. The absorbed dose values found in this way can be said to be determined in accordance with the TG-21 protocol.

Values of N_D/N_X are also given in the second row for each chamber (where N_D refers to the absorbed-dose to water calibration factor in a ^{60}Co beam and not the IAEA's equivalent of N_{gas}, which is unfortunately, also denoted N_D in the IAEA Code). This second set of N_D/N_X values is based on using the corrected AAPM equations for N_{gas}[3,10] and the IAEA data set. They are presented to demonstrate the differences between the TG-21 values and the current best estimates of these values. However, once one moves away from following the TG-21 protocol, an absorbed-dose calibration factor N_D obtained from a standards laboratory should be used directly with the k_Q values in Table I based on the IAEA data set since these are consistent with the data sets used in the standards laboratories.

By way of an historical note, the quantity $100\,k_QN_D/N_X$ [rad/R] is the corrected conceptual equivalent of the quantity C_λ used for photon dosimetry in ICRU Report 14.[11] The original C_λ factors ignored all chamber-to-chamber variations whereas the correct values range from 0.938 to 0.962 for a ^{60}Co beam.

C. Dosimetry in electron beams

The k_Q formalism can be applied to cases of electron beams as well as photon beams. Conceptually, it loses its simplicity somewhat because different quantities are involved in the ratio for k_Q for electron and photon beams and because k_Q becomes a function of both the beam quality Q and the depth of dose maximum. Furthermore, one of the main advantages of the k_Q approach is that k_Q for photon beams can be measured directly against primary standards of absorbed dose. Similar standards for electron beams are further in the future and matching beam qualities in the standards laboratories and in the clinic will be a difficult problem. Thus for electron beam dosimetry it may be preferable to determine N_{gas} from an absorbed-dose calibration factor and the use Eq. (2) as done in present approaches to determine the absorbed dose in a beam of quality Q (which is defined in terms of $\bar{E}_0$, the mean energy at the surface in the TG-21 protocol). When starting from an absorbed-dose calibration factor N_D, the value of N_{gas} is given, as shown in Eq. 5, by

$$N_{gas}=\frac{N_D}{[P_{wall}P_{repl}(\bar{L}/\rho)^{water}_{air}]_{^{60}Co}} \quad \text{(Gy/C)}. \qquad (8)$$

The values of N_{gas}/N_D are also included in Table I for

TABLE I. Various dosimetric quantities for commonly used ion chambers. The upper row for each chamber contains the values from the 1983 AAPM protocol and the second row contains the best current values using the corrected AAPM equations[3,10] and physical data in the IAEA Code of Practice. k_Q is the ratio of absorbed dose to water calibration factors under reference conditions in a beam of quality Q (specified by the TPR_{10}^{20} ratio) to that in a ^{60}Co beam. The tabulated values can be interpolated linearly in TPR_{10}^{20} with an accuracy usually better than 0.1% and no worse than 0.2%. The N_D/N_X column gives the ratio of the ^{60}Co absorbed dose to water calibration factor (in Gy/meter unit) to the exposure calibration factor free-in-air (in R/meter unit) for use if starting from an exposure calibration factor [divide by 2.58×10^{-4} to get in Gy/(C/kg) for use with N_X in (C/kg)/meter unit]. The N_{gas}/N_D column is for use in electron beam dosimetry when starting from N_D, the absorbed dose to water calibration factor. For completeness, the final column gives the value of A_{wall} used in the calculations.

Ion Chamber wall/cap	wall g/cm²	inner diam mm	k_Q TPR 0.57	0.63	0.69	0.73	0.77	0.83	N_D/N_X Gy/R	N_{gas}/N_D	A_{wall}
Capintec PR-05 0.14cc C-552/polyst	0.210	4.0	1.0011 0.9989	0.9998 0.9965	0.9985 0.9936	0.9960 0.9881	0.9869 0.9776	0.9581 0.9514	9.540E-03 9.554E-03	0.9025 0.9073	0.989 0.989
Capintec PR-05P 0.07cc mini C-552/polyst	0.210	4.0	1.0011 0.9989	0.9998 0.9965	0.9985 0.9936	0.9960 0.9881	0.9869 0.9776	0.9581 0.9514	9.530E-03 9.544E-03	0.9025 0.9073	0.988 0.988
Capintec PR-06C 0.6cc farmer C-552/polyst	0.050	6.4	1.0000 0.9980	0.9993 0.9958	0.9969 0.9914	0.9931 0.9849	0.9832 0.9738	0.9554 0.9475	9.480E-03 9.491E-03	0.8969 0.8995	0.991 0.991
Capintec PR-06C 0.6cc farmer C-552/C-552	0.050	6.4	1.0000 0.9980	0.9993 0.9958	0.9969 0.9914	0.9931 0.9849	0.9832 0.9738	0.9554 0.9475	9.587E-03 9.618E-03	0.8969 0.8995	0.984 0.984
Capintec PR-06C 0.6cc farmer C-552/PMMA	0.050	6.4	1.0000 0.9980	0.9993 0.9958	0.9969 0.9914	0.9931 0.9849	0.9832 0.9738	0.9554 0.9475	9.543E-03 9.551E-03	0.8969 0.8995	0.991 0.991
Exradin A1 2mm build-up 0.5cc Spokas C-552/C-552	0.182	9.4	1.0012 0.9990	1.0002 0.9969	0.9992 0.9944	0.9974 0.9896	0.9889 0.9798	0.9611 0.9544	9.471E-03 9.472E-03	0.9088 0.9134	0.985 0.985
Exradin A1 4mm build-up 0.5cc Spokas C-552/C-552	0.182	9.4	1.0012 0.9990	1.0002 0.9969	0.9992 0.9944	0.9974 0.9896	0.9889 0.9798	0.9611 0.9544	9.385E-03 9.385E-03	0.9088 0.9134	0.976 0.976
Exradin Shonka T1 0.05cc mini A-150/A-150	0.117	3.4	1.0002 0.9986	0.9943 0.9912	0.9857 0.9816	0.9777 0.9725	0.9665 0.9613	0.9409 0.9370	9.617E-03 9.573E-03	0.8689 0.8741	0.992 0.992
Exradin T2 0.5cc Spokas A-150/A-150	0.115	9.4	1.0002 0.9986	0.9945 0.9915	0.9864 0.9823	0.9793 0.9741	0.9687 0.9635	0.9441 0.9402	9.468E-03 9.405E-03	0.8764 0.8816	0.985 0.985
FZS TK01 0.4cc waterproof delrin/delrin	0.071	7.0	0.0000 0.9993	0.0000 0.9947	0.0000 0.9886	0.0000 0.9817	0.0000 0.9710	0.0000 0.9456	9.528E-03 9.556E-03	0.8905 0.8942	0.989 0.989
NE2505 .6cc Farmer (54-59) tufnol(PMMA)/PMMA	0.075	5.9	0.9998 0.9988	0.9973 0.9938	0.9922 0.9868	0.9871 0.9796	0.9779 0.9690	0.9521 0.9445	9.574E-03 9.583E-03	0.8874 0.8885	0.992 0.992
NE2505 .6cc Farmer (59-67) tufnol(=PMMA)/PMMA	0.075	5.9	0.9998 0.9988	0.9973 0.9938	0.9922 0.9868	0.9871 0.9796	0.9779 0.9690	0.9521 0.9445	9.555E-03 9.563E-03	0.8874 0.8885	0.990 0.990
NE2505/A .6cc Farmer (67-74) Nylon66/PMMA	0.063	5.9	1.0003 0.9988	0.9944 0.9906	0.9863 0.9815	0.9789 0.9727	0.9684 0.9617	0.9429 0.9373	9.576E-03 9.559E-03	0.8773 0.8788	0.990 0.990
NE2505/3,3A .6cc Farmer (71-79) graphite/PMMA	0.065	6.3	1.0006 0.9996	0.9981 0.9956	0.9937 0.9906	0.9886 0.9845	0.9799 0.9745	0.9538 0.9501	9.565E-03 9.555E-03	0.8918 0.8975	0.990 0.990
NE2505/3,3B .6cc Farmer (74-pres) Nylon66/PMMA	0.041	6.3	1.0012 0.9996	0.9961 0.9922	0.9890 0.9836	0.9824 0.9753	0.9721 0.9645	0.9462 0.9396	9.558E-03 9.550E-03	0.8817 0.8830	0.990 0.990
NE2515 0.2cc tufnol(PMMA)/PMMA	0.074	5.9	0.9998 0.9988	0.9973 0.9938	0.9922 0.9868	0.9871 0.9796	0.9779 0.9690	0.9521 0.9444	9.536E-03 9.544E-03	0.8874 0.8885	0.988 0.988
NE2515/3 0.2cc graphite/PMMA	0.065	6.3	1.0007 0.9996	0.9981 0.9956	0.9937 0.9906	0.9886 0.9845	0.9799 0.9745	0.9538 0.9501	9.536E-03 9.526E-03	0.8918 0.8975	0.987 0.987
NE2561 .3cc NPL Sec. Std graphite/delrin	0.090	7.4	1.0008 0.9998	0.9980 0.9957	0.9936 0.9911	0.9888 0.9857	0.9807 0.9764	0.9550 0.9525	9.504E-03 9.503E-03	0.8938 0.9006	0.984 0.984
NE2571 .6cc Farmer (79-pres) graphite/ delrin	0.065	6.3	1.0006 0.9996	0.9981 0.9956	0.9937 0.9906	0.9886 0.9845	0.9799 0.9745	0.9538 0.9501	9.572E-03 9.586E-03	0.8918 0.8975	0.990 0.990

TABLE I. (*Continued.*)

Ion Chamber wall/cap	wall	inner diam	k_Q TPR						$\frac{N_D}{N_X}$	$\frac{N_{gas}}{N_D}$	A_{wall}
	g/cm^2	mm	0.57	0.63	0.69	0.73	0.77	0.83	Gy/R		
NE2577 0.2cc graphite/delrin	0.065	6.3	1.0007 0.9996	0.9981 0.9956	0.9937 0.9906	0.9886 0.9845	0.9799 0.9745	0.9638 0.9501	9.543E-03 9.557E-03	0.8918 0.8975	0.987 0.987
NE2581 .6cc robust Farmer (80 -pres) A-150/polysty	0.040	6.3	1.0010 0.9992	0.9964 0.9928	0.9897 0.9844	0.9836 0.9763	0.9735 0.9657	0.9474 0.9407	9.494E-03 9.479E-03	0.8815 0.8843	0.990 0.990
NE2581 .6cc robust Farmer (80 -pres) A-150/PMMA	0.040	6.3	1.0010 0.9992	0.9964 0.9928	0.9897 0.9844	0.9836 0.9763	0.9735 0.9657	0.9474 0.9407	9.566E-03 9.549E-03	0.8815 0.8843	0.990 0.990
PTW N23333 30-351 .6cc Farmer 3mm cap PMMA/PMMA	0.059	6.1	0.9999 0.9988	0.9974 0.9938	0.9924 0.9868	0.9873 0.9796	0.9780 0.9690	0.9521 0.9442	9.579E-03 9.587E-03	0.8878 0.8888	0.993 0.993
PTW N23333 .6cc Farmer 4.6mm cap PMMA/PMMA	0.053	6.1	0.9999 0.9988	0.9975 0.9938	0.9925 0.9868	0.9874 0.9796	0.9780 0.9690	0.9521 0.9441	9.549E-03 9.557E-03	0.8879 0.8889	0.990 0.990
PTW N233331 .4cc Farmer PMMA/PMMA	0.142	4.7	0.9998 0.9989	0.9972 0.9938	0.9918 0.9868	0.9865 0.9798	0.9777 0.9693	0.9523 0.9452	9.575E-03 9.587E-03	0.8855 0.8867	0.990 0.990
PTW M233332 .3cc normal PMMA/PMMA	0.059	5.0	0.9999 0.9988	0.9974 0.9937	0.9923 0.9867	0.9870 0.9793	0.9776 0.9686	0.9516 0.9437	9.594E-03 9.606E-03	0.8865 0.8875	0.993 0.993
PTW M233331 1.0cc Transit PMMA/PMMA	0.059	8.0	0.9999 0.9988	0.9974 0.9938	0.9927 0.9871	0.9879 0.9801	0.9787 0.9697	0.9532 0.9453	9.544E-03 9.546E-03	0.8902 0.8913	0.992 0.992
PTW M2333641 0.3cc wproof PMMA/PMMA	0.089	5.5	0.9998 0.9988	0.9973 0.9938	0.9921 0.9868	0.9869 0.9796	0.9777 0.9690	0.9521 0.9446	9.581E-03 9.590E-03	0.8867 0.8879	0.992 0.992
SSI graph/graph	0.084	8.0	1.0008 0.9998	0.9981 0.9958	0.9938 0.9912	0.9891 0.9858	0.9809 0.9764	0.9553 0.9525	9.585E-03 9.587E-03	0.8944 0.9011	0.990 0.990
SSI A-150/A-150	0.056	8.0	1.0005 0.9988	0.9953 0.9920	0.9880 0.9833	0.9818 0.9754	0.9719 0.9650	0.9464 0.9407	9.472E-03 9.430E-03	0.8804 0.8841	0.990 0.990
Victoreen 0.3cc 30-348 PMMA/PMMA	0.060	5.0	0.9999 0.9988	0.9974 0.9937	0.9923 0.9867	0.9870 0.9793	0.9776 0.9686	0.9516 0.9437	9.594E-03 9.606E-03	0.8864 0.8875	0.993 0.993
Victoreen 1.0cc 30-349 PMMA/PMMA	0.060	8.0	0.9999 0.9988	0.9974 0.9938	0.9927 0.9871	0.9878 0.9802	0.9787 0.9697	0.9532 0.9453	9.544E-03 9.546E-03	0.8902 0.8913	0.992 0.992
Victoreen 0.6cc 30-351 PMMA/PMMA	0.060	6.1	0.9999 0.9988	0.9974 0.9937	0.9924 0.9868	0.9873 0.9796	0.9780 0.9690	0.9521 0.9443	9.580E-03 9.587E-03	0.8878 0.8888	0.993 0.993
Victoreen Radocon III 550-6, .3cc polysty/ PMMA	0.117	4.8	0.9994 0.9987	0.9949 0.9927	0.9877 0.9847	0.9806 0.9764	0.9710 0.9660	0.9465 0.9428	9.606E-03 9.596E-03	0.8762 0.8796	0.991 0.991
Victoreen Radocon II .1cc 555 -100HA delrin/none	0.529	5.0	0.0000 0.9997	0.0000 0.9940	0.0000 0.9875	0.0000 0.9806	0.0000 0.9704	0.0000 0.9463	9.561E-03 9.572E-03	0.8884 0.8943	0.990 0.990
Far West Technol. IC-17 1cc A-150/none	0.550	11.0	1.0010 0.9992	0.9976 0.9937	0.9899 0.9852	0.9834 0.9784	0.9742 0.9700	0.9517 0.9500	9.489E-03 9.405E-03	0.8726 0.8793	0.983 0.983
Far West Technol IC-17A 1cc A-150/A-150	0.143	11.0	1.0002 0.9987	0.9946 0.9915	0.9863 0.9823	0.9793 0.9743	0.9691 0.9641	0.9448 0.9413	9.449E-03 9.379E-03	0.8772 0.8827	0.984 0.984
Far West Technol IC-18 0.1cc A-150/A-150	0.183	4.6	1.0007 0.9990	0.9950 0.9918	0.9857 0.9818	0.9778 0.9730	0.9670 0.9623	0.9414 0.9384	9.619E-03 9.564E-03	0.8678 0.8737	0.991 0.991

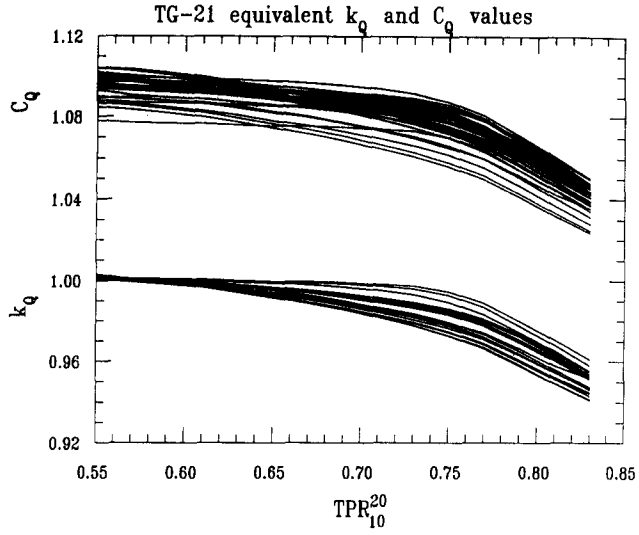

FIG. 1. Plots versus TPR_{10}^{20} of TG-21 equivalent values of k_Q and C_Q values for all chambers presented in Table I. There is a reduction in chamber to chamber variation obtained by using the k_Q approach although the functional shape for a given detector is the same in each case.

convenience. Note that these values do not depend on correcting the N_{gas} equations of the TG-21 protocol. The value in the second row for each chamber represents the current "best" estimate because it uses the most up to date data set.

III. A COMPARISON TO USE OF FREE-IN-AIR CALIBRATION FACTORS

A. The C_Q approach

To investigate the relative merits of using an absorbed-dose calibration based approach versus an in-air calibration factor based approach, one must first define the optimal approach based on the in-air calibration factors. This can best be done by starting from an air-kerma calibration factor $N_K[=N_X(\bar{W}/e)_{air}/(1-\bar{g})]$ and by defining a single factor, called C_Q, to relate the ion chamber readings in phantom M to the dose to the medium, i.e., C_Q is defined such that:

$$D_{med}=MP_{ion}N_KC_Q \quad \text{(Gy)}. \tag{9}$$

This general approach has been used in several protocols (e.g., the HPA[12] and Dutch[13] codes of practice) and is usually accompanied by requiring use of one of a few specified types of ion chambers. Using Eq. (2) for the dose to the medium, Eq. (18) in Appendix A for N_{gas} and substituting the relationship between N_K and N_X gives:

$$C_Q=\frac{(1-\bar{g})\,[P_{wall}P_{repl}(\bar{L}/\rho)^{med}_{air}]_Q}{[(\bar{L}/\rho)^{wall}_{air}(\bar{\mu}_{en}/\rho)^{air}_{wall}K_{wall}K_{comp}K^{c}_{ion}]_{^{60}Co}}. \tag{10}$$

One of the advantages of using this approach rather than the N_{gas} and N_X approach is that C_Q is within about 10% of unity.

The first thing to note is that the Q dependence of C_Q is identical to that of k_Q as can be seen by a comparison of Eq. (10) for C_Q to Eq. (6) for k_Q. However, the spread in values of C_Q is much greater than that for k_Q as can be seen in Fig. 1 which presents plots of the k_Q and C_Q values vs TPR_{10}^{20} for all the chambers listed in Table I. This is because the differences in buildup cap materials and thicknesses affect C_Q but not k_Q.

The C_Q approach is, in principle, as easy to use as the k_Q approach, especially since a table of C_Q values equivalent to Table I for the k_Q values can be produced (see Ref. 14 for such data). There are four main reasons that this approach is not as appealing as the k_Q approach.

(1) Since the C_Q approach works through the air-kerma calibration factor, it is conceptually complex and thus difficult to explain and to learn. Furthermore, the dependence of C_Q factors on the thickness and material of a buildup cap, which is not used in any of the clinical measurements in the dosimetry chain, is an unnecessary complication.

(2) The calculation of C_Q is complex, requiring knowledge of many quantities related to the air-kerma part of the equation.

(3) The uncertainty in the calculated value of C_Q is higher than that of k_Q because there are many extra factors required and knowledge is required of different quantities, not just the changes in a quantity with beam quality. For example, an error in the wall to air stopping-power ratio will have an effect on the value of C_Q whereas for k_Q the value of the wall to air stopping-power ratio enters only weakly through the P_{wall} calculations. Similarily an error in the water to air stopping-power ratios will directly affect the value of C_Q but will only have an effect on the value of k_Q if there is an error in the change in the stopping-power ratio with beam quality.

(4) The uncertainty in measuring C_Q values is much higher than that for measuring k_Q values because the full uncertainties in the primary standards for both air-kerma and absorbed dose to water are involved. In contrast, for measurement of k_Q values, only the *relative* uncertainties in the absorbed-dose to water standards are involved. However, this point must not be pushed too far. For a given chamber *using measured values* of k_Q or C_Q, only the uncertainty in the absorbed-dose standard at the beam quality of interest comes into the final uncertainty in the measured dose. The other factors all cancel out and only the uncertainty in the transfer must be taken into account, i.e. if the air-kerma standard were wrong by a factor of two, the C_Q value would be also, but the measured absorbed dose to water in the clinic would only depend on the accuracy of the primary standard for absorbed dose to water.

B. The N_{gas} approach

The C_Q approach was introduced to make use of an in-air calibration as simple as possible and analogous to the k_Q procedure in practical terms. This by-passes the equivalent, now traditional approach of the AAPM TG-21 protocol where Eq. (9) can be written:

$$D_{\text{med}}=MP_{\text{ion}}N_{\text{gas}}[P_{\text{wall}}P_{\text{repl}}(\bar{L}/\rho)^{\text{med}}_{\text{air}}]_Q \quad \text{(Gy)}, \quad (11)$$

with a corrected equation for N_{gas} given by

$$N_{\text{gas}}=\frac{N_K(1-\bar{g})}{(\bar{L}/\rho)^{\text{wall}}_{\text{air}}(\bar{\mu}_{en}/\rho)^{\text{air}}_{\text{wall}}KK^{c}_{\text{ion}}} \quad \text{(Gy C}^{-1}\text{)}, \quad (12)$$

where N_{gas} has the standard meaning but has been written in terms of the air-kerma calibration factor. In using this approach the complexities of using an in-air calibration factor are handled within the factor N_{gas}. However, all the arguments against using the C_Q approach also apply here in only a slightly modified form. Also, users in the clinic face a more complex scheme in this approach because they must determine a variety of factors [N_{gas}, P_{wall}, P_{repl}, and $(\bar{L}/\rho)^{\text{med}}_{\text{air}}$] instead of just one C_Q value. Furthermore, making measurements to confirm the N_{gas} approach is very difficult without, in effect, measuring k_Q or C_Q. Most of the factors cannot be isolated and measured [e.g., N_{gas} or $(\bar{L}/\rho)^{\text{med}}_{\text{air}}$]. There is little *practical* benefit from analyzing things in this manner. Nonetheless it continues to be important to have a theoretical treatment available which recognizes each of the components affecting the overall response and this was the real contribution of the TG-21 protocol.

IV. PLASTIC PHANTOMS IN PHOTON BEAMS

If a plastic phantom is used in a photon beam and if, as a first step in clinical dosimetry, the absorbed dose in the plastic is sought, then the conversion factor for absorbed-dose calibration factors can be thought of as having two components. One is the variation of the absorbed dose to plastic calibration factor with Q. This is just k_Q, i.e.:

$$D^{Q}_{\text{plastic}}=MP_{\text{ion}}N^{Q}_{D,\text{plastic}} \quad \text{(Gy)} \quad (13)$$

$$=MP_{\text{ion}}k_Q N^{Q_0}_{D,\text{plastic}} \quad \text{(Gy)}, \quad (14)$$

which is calculated as in the water phantom case by using Eq. (6), but using the appropriate data for the plastic medium.

The other component is the factor to convert from absorbed dose to water into absorbed dose to plastic in the calibration beam Q_0, i.e., $N^{Q_0}_{D,\text{plastic}} = k_{\text{plastic}}N^{Q_0}_{D,\text{water}}$ which leads to

$$D^{Q}_{\text{plastic}}=MP_{\text{ion}}k_{\text{plastic}}k_Q N^{Q_0}_{D,\text{water}} \quad \text{(Gy)}. \quad (15)$$

For all the chambers considered, the variation of k_Q with Q for plastics is found to be similar to that for water. For a PMMA phantom the calculated value of k_Q is within 0.1% of that for water in Table I except above a TPR^{20}_{10} value of 0.79 (20 MV) where the value of k_Q in a PMMA phantom may be as much as 0.4% less than that in water. In a polystyrene phantom the difference is somewhat larger, ranging up to 0.6% greater than the value in a water phantom in some cases.

The conversion from water to plastic absorbed-dose calibration factors is a 2% to 3% effect and is given by:

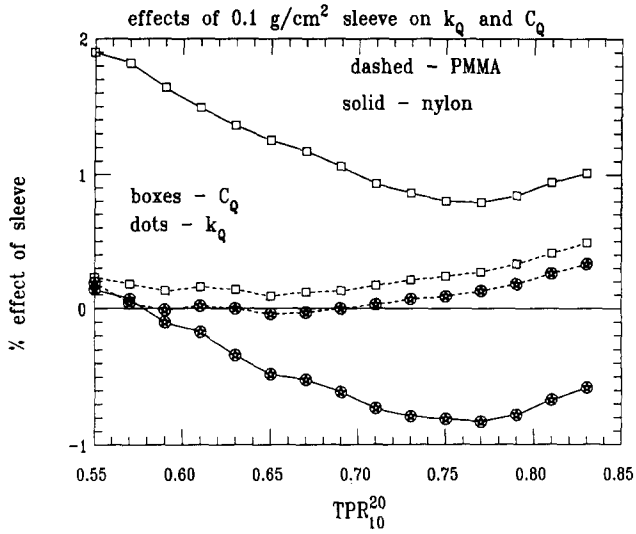

FIG. 2. Effects of 0.1 g/cm² sleeves of PMMA (dashed curves) and nylon (solid curves) on the calculated values of k_Q (shown as dots) and C_Q (shown as boxes). The k_Q approach reduces the size of the effect by a factor of about two in many cases.

$$k_{\text{plastic}}=\frac{[P_{\text{wall}}(\bar{L}/\rho)^{\text{plastic}}_{\text{air}}]_{^{60}\text{Co}}}{[P_{\text{wall}}(\bar{L}/\rho)^{\text{water}}_{\text{air}}]_{^{60}\text{Co}}}, \quad (16)$$

where the numerator is evaluated for the phantom being plastic and the denominator for it being water. This formula can be derived using Eq. (8) applied in a plastic or water phantom and it assumes, as do current protocols, that the replacement factor P_{repl} is independent of phantom material. For a PMMA phantom, k_{plastic} is within 0.1% of 0.972 (using the AAPM data set) for all the chambers in Table I. (No change is expected using the IAEA data set.) For a polystyrene phantom it ranges from 0.967 to 0.976, but this range is narrowed to within 0.3% of 0.973 for all chambers with walls less than 0.1 g/cm² thick.

In short, when seeking the dose to plastic in a plastic phantom, the values of k_Q given in Table I can be used in conjunction with the k_{plastic} values given above. In PMMA, these values correspond to the detailed TG-21 protocol values within 0.2% in most cases. In polystyrene, the discrepancies from the AAPM values are up to 0.6%. In either case, explicitly calculated values of k_Q and k_{plastic} are available for all chambers.[14]

V. EFFECTS OF WATERPROOFING SLEEVES

When using ion chambers in a water phantom it is necessary to waterproof the ion chamber. Although not discussed in most protocols, this has some effect on the ion chamber response. Extensions of the P_{wall} correction factor have been proposed[15,16] to take into account these waterproofing sleeves, especially when fairly thick walled sleeves are used [see Eq. (22) in Appendix A]. Unfortunately, the scarce experimental measurements of the effects of these sleeves is not in good agreement with these predictions.[15,17] However, one of the advantages of using the k_Q approach

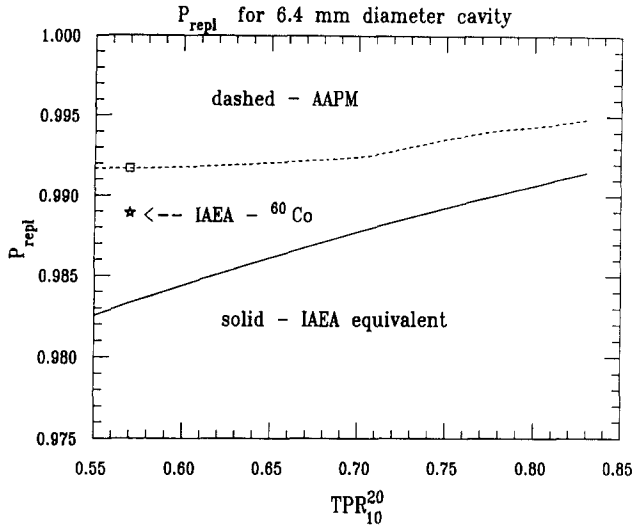

FIG. 3. Comparison of the AAPM TG-21 values of P_{repl} and the value of the equivalent correction in the IAEA Code of Practice for a 6.4-mm diameter Farmer-like chamber as a function of beam quality specified as TPR^{20}_{10}. The symbols show the values specified for ^{60}Co beams.

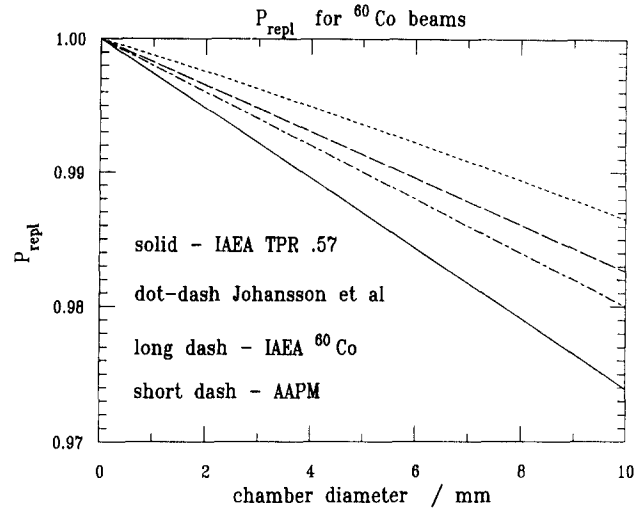

FIG. 4. Comparison, as a function of chamber diameter, of the effective values of the replacement correction factor given by a variety of approaches. The upper short-dash curve is that given by TG-21. The long dash curve is equivalent to the offset recommended by the IAEA for a ^{60}Co beam whereas the solid curve is the same quantity for a beam with a TPR^{20}_{10} value of 0.57. The dot-dash curve is based directly on the data of Johansson *et al.* upon which the IAEA approach was based.[19]

is that it reduces these effects typically by a factor of 2 because only the change in the effect of the sleeve has an effect on k_Q. Figure 2 presents the calculated effects on both k_Q and C_Q of PMMA and nylon sleeves of 0.1-g/cm^2 thickness added to a Farmer chamber with 0.05 g/cm^2 thick walls of air-equivalent plastic. Similar curves were obtained for Farmer chambers with walls of graphite and A-150 as well. The k_Q approach substantially reduces the calculated effect. Since the measured effects for nylon are much less than predicted,[17] it is clear that more work is required on this aspect of dosimetry.

VI. USING THE IAEA CODE OF PRACTICE

Up to this point all the results presented have been based on the AAPM TG-21's approach, in some cases after correcting all the errors in the equations and in some cases using the more consistent physical data presented in the IAEA Code of Practice. However, the corrected AAPM equations and the IAEA Code still differ in one important aspect. The AAPM protocol handles the effects of inserting a cavity into a phantom by using a correction factor P_{repl} whereas the IAEA Code corrects for the same effect by considering the point of measurement of the absorbed dose to be upstream of the center of the ion chamber rather than at the midpoint. As pointed out previously,[3] these corrections differ in magnitude because the basic data used to determine them by the two organizations were obtained from different approaches as well as being implemented in a different manner. Conceptually the k_Q approach deals with this issue by treating the point of measurement as the midpoint of a cylindrical chamber which means that to calculate k_Q based on the IAEA Code of Practice one must have an effective P_{repl} correction factor which is equivalent to the IAEA Code's offsets in the point of measurement. The procedure for doing this has been described elsewhere[18] and is outlined in Appendix B [see Eq. (26)]. Figure 3 shows the size of the differences between the AAPM value of P_{repl} and the effective value of P_{repl} used in the IAEA Code for a cavity diameter typical of a Farmer-like chamber. In photon beams, this is the only difference between the physics in the AAPM TG-21 protocol and IAEA Code of Practice (ignoring aluminum electrode differences, after corrections and using the same data sets). The figure also makes another crucial point concerning k_Q factors. Note that the IAEA's effective P_{repl} for ^{60}Co is *not* on the curve for the TPR^{20}_{10} values commonly found for ^{60}Co beams because the offset for ^{60}Co beams is different than for all other beams. The net effect is that k_Q values for the IAEA Code do not go to unity for TPR^{20}_{10} values near 0.57 which is a typical value for a ^{60}Co beam.

Figure 4 presents a comparison of various P_{repl} correction factors as a function of cavity diameter in a ^{60}Co beam. The upper curve is that from the TG-21 protocol. The long dashed and solid curves are those given by the IAEA offsets in the effective point of measurement as defined explicitly for a ^{60}Co beam (long dash) or assuming a general beam with TPR^{20}_{10} of 0.57 (solid). The final dashed-dot curve is the values implied by the original data of Johansson *et al.*[19] on which the IAEA's offsets are based. These are significant differences which deserve further research.

Figure 5 presents a comparison of the calculated k_Q values for the NE2561 NPL secondary standard chamber with graphite walls. The upper curve was calculated using the original AAPM TG-21 protocol, the middle curve uses the TG-21 approach with the IAEA data set and the lower curve uses the IAEA Code of Practice with the effective P_{repl} correction factor. The fact that the TG-21 and IAEA approaches converge for higher TPR^{20}_{10} values when using

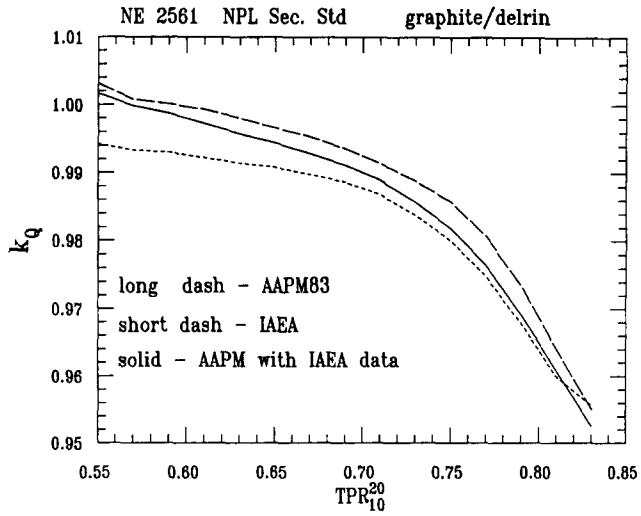

FIG. 5. Comparison of k_Q curves for an NE2561 ion chamber calculated using the original TG-21 protocol (upper long dash), the TG-21 approach but with the IAEA data set (solid curve) and using the IAEA Code of Practice (short dashed curve).

the same data sets is fortuitous. It occurs because the *ratio* of P_{repl} values in ^{60}Co beams and higher-energy beams reach the same value while the values remain different [see Fig. 3]. The k_Q values differ for lower-energy beams because of the unique offset for ^{60}Co beams in the IAEA Code. However, if this artifact were removed, there would be a significant discrepancy for higher TPR_{10}^{20} values because of the fundamental difference between TG-21 and the IAEA in approaches and data bases used to account for the effects of inserting a cavity.

Figure 5 also shows the effect of the IAEA's correction for the hollow aluminum electrode in the NE2561 (taken to be the equivalent of an 0.5-mm diameter solid electrode)

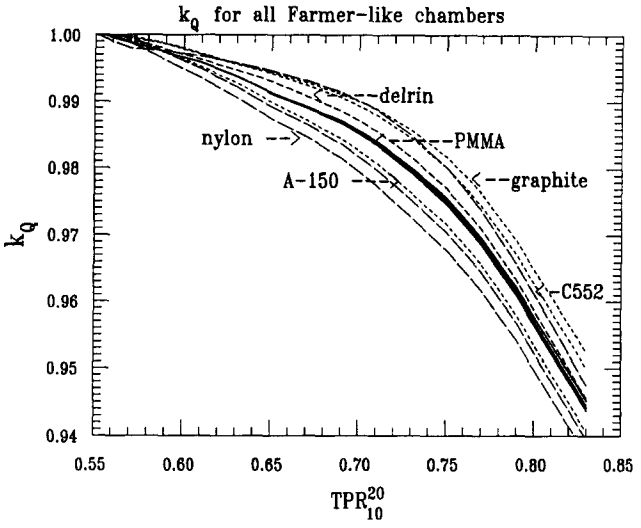

FIG. 6. Calculated k_Q factors for all 17 Farmer-like chambers in Table I. The IAEA data set and AAPM values of P_{repl} were used in the calculations. Chambers of the same material are shown by the same type of curve.

TABLE II. Values of k_Q for any chamber with walls less than 0.25 g/cm^2 for the materials shown. These values can be linearly interpolated in beam quality specified by TPR_{10}^{20}. The curves reproduce the values for all the chambers shown in Table I within the following tolerances: PMMA, delrin, ±0.1%; graphite, ±0.12%; nylon, ±0.2%; A-150, ±0.3%; C552, ±0.4%. The values in the first row for each chamber material are for the AAPM TG-21 protocol and those in the second row are for the AAPM approach with the IAEA data set. Table III gives equations for the same data.

	k_Q					
Ion chamber wall material	TPR_{10}^{20} 0.57	0.63	0.69	0.73	0.77	0.83
PMMA	0.9999	0.9974	0.9924	0.9873	0.9781	0.9523
	0.9988	0.9937	0.9868	0.9797	0.9691	0.9444
Delrin	...	...	...	...	...	...
	0.9993	0.9947	0.9886	0.9817	0.9710	0.9456
Graphite	1.0008	0.9980	0.9936	0.9886	0.9802	0.9542
	0.9998	0.9957	0.9909	0.9852	0.9755	0.9513
A-150 or nylon	1.0005	0.9949	0.9871	0.9802	0.9698	0.9442
	0.9994	0.9914	0.9824	0.9738	0.9630	0.9384
C-552	1.0010	1.0003	0.9984	0.9959	0.9868	0.9584
	0.9990	0.9971	0.9934	0.9881	0.9780	0.9514

which is accounted for using a correction called p_{cel} in the IAEAs dose equation. In photon beams, the correction only applies to photon beams above 25 MV and causes a 0.4% increase in k_Q.

For all the ion chambers discussed here[14] a complete compilation is available of k_Q, C_Q, and other dosimetric quantities, calculated using the IAEA Code of Practice.

VII. A UNIVERSAL k_Q CURVE?

Table I presents k_Q data for many different chambers, but as can be seen from Fig. 1, the maximum variation is

TABLE III. Values of k_Q as given by the equation: $k_Q = 1 + a_1(TPR - 0.57) + a_2(TPR - 0.57)^2 + a_3(TPR - 0.57)^3$, for any chamber with walls less than 0.25 g/cm^2 for the materials shown. The values in the first row for each chamber material are for the AAPM TG-21 protocol and those in the second row are for the AAPM approach with the IAEA data set.

	$k_Q = 1 + a_1(TPR-0.57) + a_2(TPR-0.57)^2 + a_3(TPR-0.57)^3$		
Ion Chamber wall material	a_1	a_2	a_3
PMMA	−0.0627	0.4702	−3.616
	−0.1257	0.5233	−3.354
Delrin	...	...	...
	−0.1039	0.4797	−3.439
Graphite	−0.0877	0.5279	−3.536
	−0.0536	0.4871	−3.686
A-150	−0.1068	0.3628	−3.025
	−0.1656	0.5035	−2.988
Nylon	−0.0816	0.1461	−2.532
	−0.1588	0.4255	−2.820
C-552	−0.0296	0.8135	−5.084
	−0.0770	0.7125	−4.408

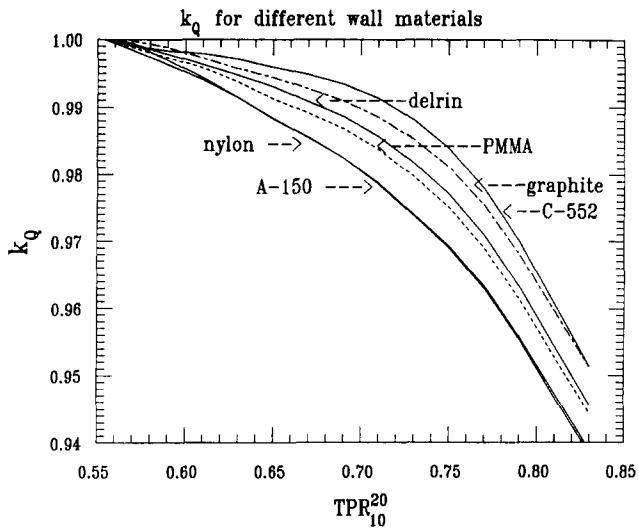

FIG. 7. Universal k_Q curves for all chambers of walls of the indicated materials and thicknesses less than 0.25 g/cm^2. These curves agree with the tabulated IAEA values for all such chambers in Table I to within 0.1% to 0.4%, depending on the material (see caption of Table II for specific tolerances).

only 2%. Thus, with an accuracy of ±1%, it is possible to adopt a single, "universal" k_Q curve for all chambers in Table I. This range may be somewhat larger than tolerable. Figure 6 presents k_Q curves for a more restricted situation, namely for Farmer-like chambers. In this case there is only a ±0.7% variation about a "neutral" median value. This is given accurately by any of the PMMA-walled Farmer chambers in Table I which are what make up the dark central group in Fig. 6.

Alternatively, the formula:

$$k_Q(Q) = 1.0 - 0.0215(\mathrm{TPR} - 0.57) - 0.736(\mathrm{TPR} - 0.57)^2 \quad (17)$$

reproduces the data for a water-walled (i.e., wall-less) chamber with a diameter of 6.4 mm to within 0.25% and is within 1% of all the IAEA based data in Table I. Figure 6 also differentiates detectors by wall material and, as the figure makes clear, the curves for any particular wall material are very similar. This occurs because the only significant variation between curves comes through the P_{wall} factor in Eq. (6) and this depends only weakly on the wall thickness. With this in mind, k_Q curves have been defined for each wall material. These curves, which are shown in Fig. 7, are applicable to all chambers with those walls and a wall thickness less than 0.25 g/cm^2. They match the values for each specific chamber within tolerances of 0.1% to 0.4% as specified in the caption of Table II. Table III presents the coefficients of a cubic fit to the same data as presented in Table II. Use of these curves is clearly acceptable for practical dosimetry since there is an underlying uncertainty in the absorbed dose of 0.5% to 0.8% based on the systematic uncertainty in the primary standards of absorbed dose.

VIII. SUMMARY AND CONCLUSIONS

This paper argues that clinical external beam dosimetry protocols are greatly simplified by basing them on absorbed-dose calibration factors for ion chambers. Tables of calculated k_Q values and N_D/N_X factors are presented and allow this simplified approach to be followed immediately for photon beams while still rigorously conforming to the values in the TG-21 protocol. A second set of values is presented which is based on the latest physical data (in particular stopping-power ratios and ratios of mass energy absorption coefficients from the IAEA Code of Practice) and the corrected AAPM equations [the corrections only affect the values of N_D/N_X (Refs. 3 and 10), not values of k_Q nor N_{gas}/N_D].

The new primary standards of absorbed dose which are being developed in a variety of primary standards laboratories for accelerator photon beams will allow accurate measurement of k_Q factors for a wide variety of chambers. An inherent assumption in all current dosimetry protocols is that ion chambers of a given construction all behave in the same manner, and this assumption is implied by the use of k_Q factors as well. This is not necessarily the case and with the development of facilities which can provide explicit calibrations in accelerator beams, one may find some chamber-to-chamber variation in k_Q. It is thought that this is unlikely and it is usually easier to detect faulty or unusual behavior using a soft x-ray calibration. Nonetheless, possible high-energy variation will be detected using high-energy absorbed-dose calibrations.

In electron beams, because of the stronger dependence of absorbed-dose calibration factors on beam quality and because of possible problems matching beam qualities in the clinic with those in the standards laboratory, the best approach to electron beam dosimetry may be to use a revised N_{gas} approach in which N_{gas} is determined from a ^{60}Co absorbed-dose to water calibration factor using Eq. (8). The required N_{gas}/N_D ratios are included in Table I.

The approach in this paper has been developed in the context of the TG-21 protocol and hence photon beam quality has been specified in terms of TPR^{20}_{10} ratios. This is not essential to the arguments and there are indications that specification of beam quality in terms of percentage depth dose at 10 cm may be more appropriate.[20,21]

One advantage of adopting protocols based on absorbed-dose standards is that exposure or air-kerma standards would become redundant from the point of view of external beam radiotherapy.

The major advantage of using a protocol based on absorbed-dose calibration factors is the much simpler physical principles involved. By starting from a consideration of the change in the absorbed-dose calibration factor with beam quality in the form of a single factor k_Q the conceptual and practical aspects of clinical dosimetry are greatly simplified. Hence, fewer errors will be made and significant improvements in routine clinical dosimetry can be expected.

ACKNOWLEDGMENTS

I wish to thank Dr. Klaus Hohlfeld of the PTB in Germany who patiently convinced me of the advantages of absorbed-dose calibration factors and the k_Q approach. The parts of this paper devoted to a discussion of the general approach are mostly the ideas he presented to me, but translated into the context of the AAPM's TG-21 protocol. As always, I thank my colleagues at NRC for many lively discussions, especially Carl Ross.

APPENDIX A: THE BASIC EQUATIONS OF THE AAPM PROTOCOL

To emphasize their complexity and to provide a clearly defined notation, the following is a summary of the equations required to use the AAPM protocol. The equations are those of the AAPM TG-21 protocol[1,22] but with the various errors removed (see formulation A in Ref. 10 for a derivation, or Ref. 3 for a simplified derivation). The same equations are the basis of other protocols[2] but with different notation.

The protocols start by defining a chamber-specific cavity-gas calibration factor which can be shown to be given by

$$N_{\text{gas}}=\frac{N_X(W/e)_{\text{air}}}{(\bar{L}/\rho)^{\text{wall}}_{\text{air}}(\overline{\mu_{\text{en}}}/\rho)^{\text{air}}_{\text{wall}}KK^c_{\text{ion}}} \quad (\text{Gy C}^{-1}), \tag{18}$$

where N_X is the exposure calibration factor of the ion chamber (kg^{-1}), $(W/e)_{\text{air}}$ is the energy deposited per unit charge released by electrons slowing in *dry* air (J/C), $(\bar{L}/\rho)^{\text{wall}}_{\text{air}}$ is the stopping-power ratio in the calibration beam, $(\overline{\mu_{\text{en}}}/\rho)^{\text{air}}_{\text{wall}}$ is the ratio of mass energy absorption coefficients in the calibration beam, K^c_{ion} corrects for incomplete charge collection in the calibration beam and K is the product of correction factors which all apply in the calibration beam, and is given by

$$K=K_{\text{wall}}K_{\text{pn}}K_{\text{st}}K_{\text{el}}K_{\text{comp}}, \tag{19}$$

where K_{wall} corrects for scatter and attenuation in the chamber wall, K_{pn} corrects for the axial nonuniformity of the beam, K_{st} corrects for scatter from the detector stem, and K_{el} and K_{comp} correct for any nonwall equivalent materials in the detector's central electrode and the rest of the chamber (with cap), respectively. For a buildup cap outside the chamber wall, one has

$$K_{\text{comp}}=\frac{\alpha(\bar{L}/\rho)^{\text{wall}}_{\text{air}}(\overline{\mu_{\text{en}}}/\rho)^{\text{air}}_{\text{wall}}+(1-\alpha)(\bar{L}/\rho)^{\text{cap}}_{\text{air}}(\overline{\mu_{\text{en}}}/\rho)^{\text{air}}_{\text{cap}}}{(\bar{L}/\rho)^{\text{wall}}_{\text{air}}(\overline{\mu_{\text{en}}}/\rho)^{\text{air}}_{\text{wall}}}, \tag{20}$$

where α is the fraction of the ionization in the cavity due to electrons originating in the chamber wall and $(1-\alpha)$ is the fraction from the buildup cap. The dose to the medium in the phantom is given by

$$D_{\text{med}}=MN_{\text{gas}}(\bar{L}/\rho)^{\text{med}}_{\text{air}}P_{\text{ion}}P_{\text{repl}}P_{\text{wall}} \quad (\text{Gy}), \tag{21}$$

where M is the temperature and pressure corrected ion chamber reading (C), P_{ion} corrects for lack of complete ion collection in the clinical beam, P_{wall} corrects for the fact that the ion chamber wall and water-proofing sleeve are not the same material as the phantom and is given by

$$P_{\text{wall}}=\frac{\alpha(\bar{L}/\rho)^{\text{wall}}_{\text{air}}(\overline{\mu_{\text{en}}}/\rho)^{\text{med}}_{\text{wall}}+\tau(\bar{L}/\rho)^{\text{sleeve}}_{\text{air}}(\overline{\mu_{\text{en}}}/\rho)^{\text{med}}_{\text{sleeve}}+(1-\alpha-\tau)(\bar{L}/\rho)^{\text{med}}_{\text{air}}}{(\bar{L}/\rho)^{\text{med}}_{\text{air}}}, \tag{22}$$

where α and τ are the fractions of the ionization in the cavity due to electrons set in motion in the wall and the sleeve material, respectively;[15,16] and the replacement correction factor, P_{repl}, takes into account the changes in the electron spectrum at the point of measurement because of the presence of the cavity of the ion chamber, and is given by

$$P_{\text{repl}}=P_{\text{gr}}P_{\text{fl}}, \tag{23}$$

where P_{gr} is a gradient correction factor which is needed in photon beams (but not at $d_{\max}$ in an electron beam) and P_{fl} is an electron fluence correction factor which is not needed in photon beams past $d_{\max}$ but which is needed in electron beams where it is only known at $d_{\max}$.

The dose equations above are very similar to those of the AAPM protocol with the slight extension to include a waterproofing sleeve in a water phantom. The N_{gas} equation is different from the original equation which used (W/e) for humid rather than dry air and had $K=K_{\text{wall}}K_{\text{comp}}/\beta_{\text{wall}}$.

The IAEA Code of Practice uses the same equations in another notation to obtain N_{gas} (called N_D) with the exception that it uses what amounts to a different formula for K_{comp}. The IAEA's equation for k_m is, in the current notation:

$$k_m=\alpha(\bar{L}/\rho)^{\text{air}}_{\text{wall}}(\overline{\mu_{\text{en}}}/\rho)^{\text{wall}}_{\text{air}}+(1-\alpha)\times(\bar{L}/\rho)^{\text{air}}_{\text{cap}}(\overline{\mu_{\text{en}}}/\rho)^{\text{cap}}_{\text{air}}, \tag{24}$$

which is equivalent to using:

$$K_{\text{comp}}^{\text{IAEA}} = \frac{1}{(L/\rho)_{\text{air}}^{\text{wall}}(\overline{\mu_{\text{en}}}/\rho)_{\text{wall}}^{\text{air}}[\alpha(L/\rho)_{\text{wall}}^{\text{air}}(\overline{\mu_{\text{en}}}/\rho)_{\text{air}}^{\text{wall}} + (1-\alpha)(L/\rho)_{\text{cap}}^{\text{air}}(\overline{\mu_{\text{en}}}/\rho)_{\text{air}}^{\text{cap}}]}. \quad (25)$$

Despite the difference in appearance, this formula gives the same (within 0.05%) numerical values as the AAPM equation given above as Eq. (20) and reduces to the same form exactly for $\alpha=0$ or 1.

The IAEA uses an effective point of measurement concept in its dose equation to account for P_{gr} (see below) and a correction to account for the effects of an aluminum electrode if it exists.

APPENDIX B: THE PROGRAM PROT

The program PROT is a general purpose utility which provides on-line access to all the data related to photon beam dosimetry protocols. It includes the data bases used in the AAPM protocol and the IAEA Code. Values of various quantities are presented for four different options: (i) the original AAPM equations and data base; (ii) the corrected AAPM equations from Refs. 3 and 10 as presented in Appendix A (including the IAEA's form of K_{comp}) with the AAPM database; (iii) the equations as in option (ii) but using the IAEA data base; and (iv) the IAEA formulation and data base. The program presents a wide variety of parameters such as: α, $(L/\rho)_{\text{med2}}^{\text{med1}}$, $(\overline{\mu_{\text{en}}}/\rho)_{\text{med2}}^{\text{med1}}$, P_{wall}, P_{repl}, K_{comp}, k_Q, and C_Q as a function of beam quality indicators such as TPR_{10}^{20} or NAP or other quantities such as cavity radius where appropriate. It also calculates other parameters such as N_{gas}/N_X, k_m and conversions between NAP and TPR_{10}^{20}.

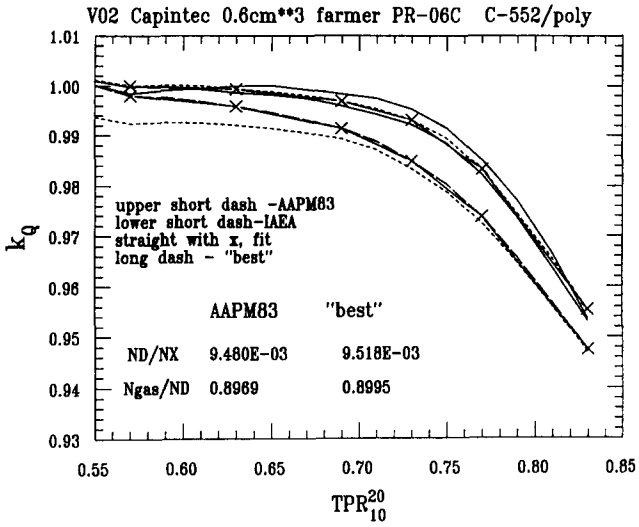

FIG. 8. Typical plot of calculated k_Q values produced by the program PROT. Values of k_Q for a water phantom are calculated using the original AAPM protocol (upper short dashed curve), the IAEA Code of Practice (lower short dashed curve) and the AAPM formulation using the IAEA data set (long dashed curve). The values from Table I are shown as $\times$ and joined by straight lines to demonstrate the accuracy of linearly interpolating the values in Table I. The two upper solid curves are the k_Q values calculated in polystyrene (top) and PMMA. N_D/N_X values are based on Eq. (7) and are in Gy/R. N_{gas}/N_D values are based on Eq. (8). The AAPM83 values are from the original protocol and the "best" estimates use the corrected AAPM equations[3,10] and the IAEA data set.

Figure 8 shows an example of the summary plots produced by the program PROT for each chamber in Table I. The plot includes three k_Q curves calculated for a water phantom plus the values tabulated in Table I to demonstrate the accuracy of the linear interpolation of these tabulated values. Curves of k_Q calculated for polystyrene and PMMA phantoms by using the original AAPM protocol are also shown to elucidate differences between k_Q values in different phantoms. The plot also includes several important conversion factors calculated using the original protocol or the corrected AAPM equations and the IAEA data set. Ref. 14 contains a figure for each chamber listed in Table I.

Several comments are required about the program.

As a check of at least part of the program, it calculates $N_{\text{gas}}/(N_X A_{\text{ion}})$ values using either the original protocol equations and data or the corrected equations with the IAEA data which is equivalent to the IAEA results in this situation. In the former case, agreement was obtained with all 27 of the Gastorf *et al.* values[9] and in the latter case, agreement was obtained with the $k_m k_{\text{att}}$ values presented in the IAEA Code of Practice.

The program produces k_Q values for the IAEA Code by calculating an effective P_{repl} correction factor which accounts for the IAEA Code's use of an effective point of measurement. This effective P_{repl} factor has been described previously[18] and is based on the fact that depth-dose curves fall off exponentially. Hence, the effect of moving the effective point of measurement by a fixed fraction of the chamber radius can be determined from a knowledge of the beams value of TPR_{10}^{20}. The effective replacement correction factor in photon beams is given by:

$$P_{\text{repl}}^{\text{IAEA}} = 1 - \left(\frac{1}{10}\ln\frac{D_{20}}{D_{10}}\right)(z_{\text{eff}} - z), \quad (26)$$

where $z_{\text{eff}}-z$ is the offset of the effective point of measurement in the IAEA Code of Practice and D_{20} and D_{10} are the relative depth dose values at 20 and 10 cm in a diverging beam with an SSD of 100 cm. This ratio of doses is given as a function of TPR_{10}^{20} in Table XIII of the IAEA Code and is included in the program.

All graphical data were determined by digitizing the graphs in the AAPM protocol[1] or letter of clarification.[22]

In calculating α, the fraction of ionization from a chamber wall, no low-energy cutoff is used (which is contrary to the suggested procedure made by the TG-21 protocol for convenience) and values are interpolated linearly to zero wall thickness. For $\text{TPR}_{10}^{20} < 0.57$, ^{60}Co data are used. For higher energy beam qualities, the values from the figure are interpolated linearly in MV and in wall thickness. The

values of α in the IAEA Code of Practice were taken to be the same as in the AAPM protocol although, as pointed out by Huq and Nath,[23] the IAEA values appear to be offset by 0.05 in the TPR_{10}^{20} axis. This should have a negligible effect on the values of P_{wall}.

Values of P_{wall} were calculated using the Shiragai[24] or Almond and Svensson formulae[25] and no difference greater than 0.05% was found in any of the cases investigated. Similarly, no significant numerical differences were found between the AAPM and IAEA formulations of K_{comp} or k_m. See Ref. 3 for a complete discussion of the differences in these formulae.

In several cases there were discrepancies found in the AAPM protocol for ratios of mass-energy absorption coefficients and stopping-power ratios between the ^{60}Co values in its Table I and the values in its Tables IV and IX for various beams specified by MV. The values in Table I were used for ^{60}Co values in air and those in its Tables IV and IX for other cases. The value of the ratio of graphite to air mass-energy absorption coefficients in TG-21's Table IX for 2-MV photon beams, is 0.5% low compared to the ^{60}Co value. This leads to considerable discrepancy for graphite-walled chambers, in particular causing k_Q to be >1 for beam's with TPR_{10}^{20} values consistent with a ^{60}Co beam. Similarly there are some minor inconsistencies in the IAEA data sets since the values of $s_{m,air}$ and $(\overline{\mu_{en}}/\rho)_{air}^{med}$ for ^{60}Co do not correspond to the same value of the TPR_{10}^{20} ratio for all materials.

For the AAPM protocol, P_{repl} for $TPR_{10}^{20}<0.57$ is treated as being in a ^{60}Co beam.

With the AAPM data set, the stopping-power ratios are taken from TG-21'sTable IX for all P_{wall} calculations and from a digitization of the revised Fig. 2 in the AAPM letter of clarification[22] for use in the dose to medium equation. The values in Table IX of the protocol show an unusual behavior between 20 and 45 MV which leads to a shoulder appearing in plots vs TPR_{10}^{20} above $TPR_{10}^{20}=0.79$. For the K_{comp} equations, the stopping-power ratios in Table I of the protocol are used.

[1]AAPM TG-21, "A protocol for the determination of absorbed dose from high-energy photon and electron beams," Med. Phys. **10**, 741–771 (1983).

[2]IAEA, "Absorbed dose determination in photon and electron beams; An inter-national code of practice" Tech. Report Series #277 (IAEA, Vienna, 1987).

[3]D. W. O. Rogers, "Fundamentals of high energy x-ray and electron dosimetry protocols," in *Advances in Radiation Oncology Physics*, edited by Jim Purdy, Medical Physics Monograph 19 (AAPM, New York, 1992), pp. 181–223.

[4]W. H. Henry, "The NRC absorbed dose to water calibration service," NRC Flyer 1977.

[5]K. Hohlfeld, "The standard DIN 6800: Procedures for absorbed dose determination in radiology by the ionization method," in *Dosimetry in Radiotherapy* Vol I, 13-24 (IAEA, Vienna, 1988).

[6]HPA, "Code of practice for high-energy photon therapy dosimetry based on the NPL absorbed dose calibration service," Phys. Med. Biol. **35**, 1355–1360 (1990).

[7]D. W. O. Rogers, "New dosimetry standards," in *Advances in Radiation Oncology Physics*, edited by Jim Purdy, Medical Physics Monograph 19 (AAPM, New York, 1992), pp. 90–110.

[8]"ICRU report committee activities," in ICRU News, June 1990 p. 20. (ICRU, Bethesda, MD).

[9]R. Gastorf, L. Humphries, and M. Rozenfeld, "Cylindrical chamber dimensions and the corresponding values of A_{wall} and $N_{gas}/(N_X A_{ion})$," Med. Phys. **13**, 751–754 (1986).

[10]D. W. O. Rogers and C. K. Ross, "The role of humidity and other correction factors in the AAPM TG-21 dosimetry protocol," Med. Phys. **15**, 40–48 (1988).

[11]ICRU Report 14, "Radiation dosimetry: X-rays and gamma-rays with maximum photon energies between 0.6 and 50 MeV," International Commission on Radiation Units and Measurements (Bethesda, MD, 1969).

[12]HPA, "Revised code of practice for dosimetry of 2 to 35 MV x-rays and of ^{137}Cs and ^{60}Co γ-ray beams," Phys. Med. Biol. **28**, 1097–1104 (1983).

[13]NCS, "Code of practice for the dosimetry of high-energy photon beams," NCS Report 2, Dec. 1986 (NCS, Bilthoven, The Netherlands).

[14]D. W. O. Rogers, "Compilation of quantities associated with dosimetry protocols," NRC Report PIRS 291, Ottawa, December 1991.

[15]W. F. Hanson, J. A. D Tinoco, "Effects of plastic protective caps on the calibration of therapy beams in water," Med. Phys. **12**, 243–248 (1985).

[16]M. T. Gillin, R. W. Kline, A Niroomand-Rad, and Daniel F. Grimm, "The effect of thickness of the waterproofing sleeve on the calibration of photon and electron beams," Med. Phys. **12**, 234–236 (1985).

[17]C. K. Ross and K. R. Shortt, "The effects of water-proofing sleeves on ionization chamber response," Phys. Med. Biol. **37**, 1403–1411 (1992).

[18]D. W. O. Rogers and C. K. Ross, "Comments on comparison of IAEA 1987 and AAPM 1983 protocols for dosimetry calibration of radiotherapy beams," Med. Phys. **19**, 213–214 (1992).

[19]K. A. Johansson, L. O. Mattsson, L. Lindborg, and H. Svensson, "Absorbed-dose determination with ionization chambers in electron and photon beams having energies between 1 and 50 MeV," IAEA Symposium Proceedings (Vienna) IAEA-SM-222/**35**, 243–270 (1977).

[20]P. D. LaRiviere, "The quality of high-energy x-ray beams," Br. J. Rad. **62**, 473–481 (1989).

[21]A. Kosunen and D. W. O. Rogers, "Beam quality specification for photon beam dosimetry," Med. Phys. **19**, 774 (1992).

[22]R. J. Schulz, P. R. Almond, G. Kutcher, R. Loevinger, R. Nath, D. W. O. Rogers, N. Suntheralingham, K. A. Wright, and F. M. Kahn, "Clarification of the AAPM task group 21 protocol," Med. Phys. **13**, 755–759 (1986).

[23]M. S. Huq and R. Nath, "Comparison of IAEA 1987 and AAPM 1983 protocols for dosimetry calibration of radiotherapy beams," Med. Phys. **18**, 26–35 (1991).

[24]A. Shiragai, "A proposal concerning the absorbed dose conversion factor," Phys. Med. Biol. **23**, 245–252 (1978).

[25]P. R. Almond and H. Svensson, "Ionization chamber dosimetry for photon and electron beams. Theoretical considerations," Acta Radiol. Ther. Phys. Biol. **16**, 177 (1977).